Passive Velocity Field Control of Mechanical Manipulators

Perry Y. Li, *Member, IEEE,* and Roberto Horowitz, *Member, IEEE*

***Abstract*—Two concepts are advocated for the task specification and control of mechanical manipulators:**

1) **coding tasks in terms of velocity fields;**
2) **designing controllers so that the manipulator when under feedback control, interacts in an energetically passive manner with its physical environment.**

Based on these two concepts, a new passive velocity field controller (PVFC) is proposed which mimics the behavior of a passive energy storage element, such as a flywheel or a spring. It stores and releases energy while interacting with the manipulator, but does not generate any. The controller has the interesting property that it stabilizes *any* multiple (positive or negative) of the desired velocity field, and exponentially stabilizes the particular multiple of the desired velocity field which is determined by the total kinetic energy of the manipulator control system.

***Index Terms*—Contour following, mechanical systems, passivity, velocity field.**

NOTATIONS

OBJECTS in a manifold are denoted by unbold letters or symbols. Their local coordinate representations are denoted by bold letters and symbols. Thus if $q \in \mathcal{G}$, and $\mathcal{G}$ is a n-dimensional configuration manifold, then $\mathbf{q} = [q_1, q_2, \ldots, q_n]^T \in \Re^n$ represents the local coordinates of q. Both the so called joint coordinates and the workspace coordinates can be used as the local coordinates of the manipulator configuration, $\mathcal{G}$. Generally capital letters will be used to denote *desired* quantities and lower case letters to denote *actual* quantities.

I. INTRODUCTION

Traditionally, robot tasks are defined by specifying desired timed trajectories in the manipulator's workspace, which the manipulator is required to track at every instant of time. However, in many applications, the actual timing in the desired trajectory is unimportant, compared to the coordination and synchronization requirements between the various degrees of freedom. A contour following task, such as requiring a robot to draw a figure in Cartesian space, falls into this category. In the traditional timed trajectory approach, the *desired contour* is parameterized as a function of time $Q : \Re_+ \to \mathcal{G}, t \mapsto Q(t)$, where $\mathcal{G} = \{q\}$ is the n-dimensional configuration manifold. Let the actual trajectory of the manipulator be $q : \Re_+ \to \mathcal{G}$. The design goal of a trajectory tracking controller consists in making the trajectory tracking error $q(t) - Q(t)$ converge to 0 as $t \to \infty$.

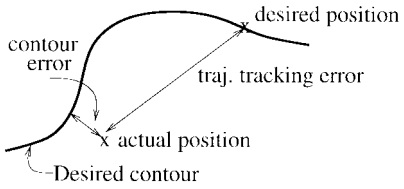

Fig. 1. Tracking error and contouring error.

As pointed out in [1] and others, the trajectory tracking error does not reflect how well the contour is being followed. For example, the actual position and the desired location could just be out of step by a time interval Δt, i.e., $q(t - \Delta t) - Q(t) = 0$. If timing is not critical, there is no need to keep up with the desired timed trajectory. On the other hand, controllers that try to minimize the trajectory tracking error, $q(t) - Q(t)$, may in fact cause the robot to leave the contour to catch up with the desired location specified by the timed trajectory. This can cause a phenomenon known as *radial reduction* in which the actual path traced out has a smaller radius than the one specified by the desired trajectory $Q(t)$. This highlights the fact that "contour error" (Fig. 1) which actually measures the distance between the actual position and the contour is a more appropriate way to describe whether the contour is being followed, than the traditional trajectory tracking error.

Contour following tasks can be effectively encoded through the use of *desired* velocity fields. Let $T_q\mathcal{G}$ be the tangent space of $\mathcal{G}$ at the specific manipulator configuration q. A (time invariant) *desired* velocity field (or a vector field) V is a map

$$V : \mathcal{G} \to T\mathcal{G}; \quad q \mapsto V(q) \in T_q\mathcal{G}$$

where $T\mathcal{G} = \cup_{q \in \mathcal{G}} T_q\mathcal{G}$ is the tangent bundle of $\mathcal{G}$ [2]. Thus, the desired velocity field defines a tangent vector (the desired velocity) at every point of the configuration space. Roughly speaking, a velocity field would encode a contour if $V(q)$ points toward the contour, and is tangent to it whenever q belongs to the contour. Fig. 2 shows a desired velocity field for the task of tracing a circle on a rectangular configuration space.

Manuscript received August 19, 1996; revised April 25, 1999. This paper was recommended for publication by Associate Editor A. Burdea and Editor A. De Luca upon evaluation of the reviewers' comments.

P. Y. Li is with the Department of Mechanical Engineering, University of Minnesota, Minneapolis, MN 55455 USA (e-mail: pli@me.umn.edu).

R. Horowitz is with the Department of Mechanical Engineering, University of California, Berkeley, CA 94720-1740 USA (e-mail: horowitz@me.berkeley.edu).

Publisher Item Identifier S 1042-296X(99)06232-1.

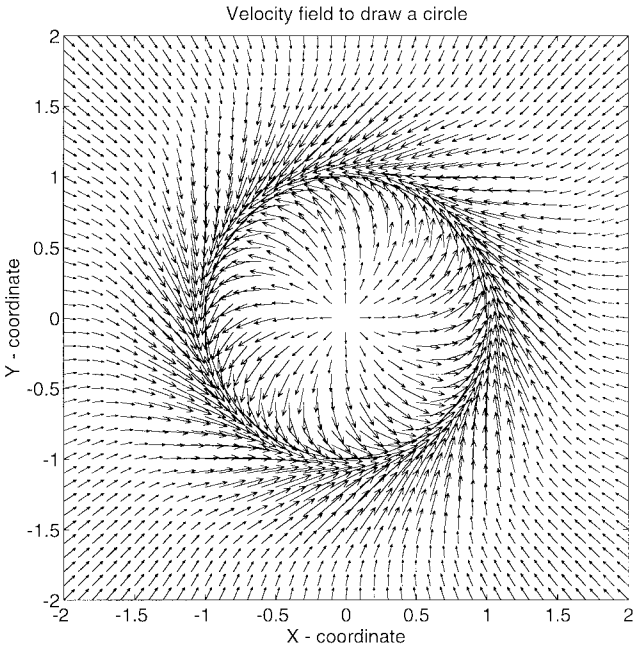

Fig. 2. Velocity field for tracing a circle.

Given a specific desired velocity field V, we define the α-related velocity field error as

$$e_\alpha(t) = \dot{q}(t) - \alpha V(q(t))$$

where $\dot{q}(t) \in T_{q(t)}\mathcal{G}$ is the manipulator's actual velocity and $\alpha > 0$ is a constant. The velocity field tracking control objective is to cause $e_\alpha(t) \to 0$ for some α. Notice that if $e_\alpha(t) \equiv 0$, the manipulator travels in the direction of $V(q(t))$ so that the ODE $\dot{q} = \alpha V(q)$ is satisfied. If, in addition, $V(q)$ also encodes a desired contour, then the manipulator will converge to and follow the contour. Moreover, the speed at which the manipulator follows the contour will be proportional to the constant α. In this way, an entire set of contour following tasks which differ from each other only in the speed at which the prescribed contour is followed is encoded by the same desired velocity field $V(q)$.

It is also possible to encode a timed trajectory tracking task using a *time varying* desired velocity field. Let $Q : \Re_+ \to \mathcal{G}$ be a desired timed trajectory and $d : \mathcal{G} \times \mathcal{G} \to \Re_+$ be a distance measure on $\mathcal{G}$. An associated *time varying* velocity field $V : \mathcal{G} \to T\mathcal{G}$ for $Q(t)$ can be defined as

$$V(q,t) = \dot{Q}(t) - \zeta \cdot \mathrm{grad}(d(Q(t),q)), \tag{1}$$

where $\zeta > 0$ is a constant and $\mathrm{grad}(d(Q(t),q))$ is the gradient vector field of the distance measure d with respect to q while keeping $Q(t)$ constant (see [3] for details). This definition is closely related to the so called sliding surface or reference velocity error signal in [4], [5], which is instrumental in developing stable passivity based trajectory tracking controllers for robot manipulators. Indeed, if we assume that $\mathcal{G} = \Re^n$ and d is the Euclidean norm, then $V(q,t)$ is the reference velocity error signal given by

$$V(q,t) = \dot{Q}(t) - \zeta(q(t) - Q(t)) \quad \zeta > 0. \tag{2}$$

Hence, by tracking the desired velocity field $V(q,t)$, the timed trajectory $Q(t)$ will also be tracked. However, in this paper we will mostly consider the case where the desired velocity field is time invariant.

Related to task specification using velocity fields is the event based robot planning/control strategy presented in [6]. In [6], a robotic task is represented by a path parameterized in terms of a scalar called the "*task variable*". The control algorithm is designed to track the location specified by the task variable. The dynamics of the task variable is nominally that of time t and is modified when the robot's sensors detect unusual circumstances, such as the presence of an obstacle. Because the control scheme in [6] is essentially hierarchical, it may not be able to deal with *undetected* or unmodeled disturbances since the dynamics of the task variable will be unaffected by the current state of the robot in these circumstances. In comparison, when the contour following task is encoded in terms of a velocity field, instead of specifying the target position, a desired velocity based on the robot *current* location is specified. Thus, with an appropriately designed velocity field, the robot will converge to the desired contour in a manner best suited for its current location.

The second concept advocated in this paper is the use of controllers that maintain an energetically passive relationship between the manipulator under closed loop control and its physical environment, while causing the manipulator to perform the desired task.

Definition 1 [7]: A dynamic system with input $u \in \mathcal{U}$ and output $y \in \mathcal{Y}$ is passive with respect to the supply rate $s : \mathcal{U} \times \mathcal{Y} \to \Re$ if, for any $u : \Re_+ \to \mathcal{U}$ and any $t \geq 0$, the following relationship is satisfied

$$\int_0^t s(u(\tau), y(\tau))\, d\tau \geq -c^2$$

where $c \in \Re$ depends on the system's initial conditions.

Mechanical manipulators are subjected to two types of inputs: control inputs τ, and external forces τ_e. The former are the torques or forces generated by the actuators, while the latter are disturbances or contact forces encountered when the manipulator is interacting with an object. τ and τ_e will be modeled as elements of $T^*\mathcal{G}$, the cotangent bundle of $\mathcal{G}$ [8].

Let us consider the total forces acting on the manipulator, $\tau_{\mathrm{tot}} = \tau + \tau_e$, to be the input to the manipulator, and the manipulator's velocity $\dot{q}$ to be its output. There is a natural supply rate for this input/output system which is the total mechanical power input, given by the action of τ_{tot} on $\dot{q}$. In coordinates, it is represented by $s(\tau_{\mathrm{tot}}, \dot{q}) = \boldsymbol{\tau}_{\mathrm{tot}}^T \dot{\mathbf{q}}$, where $(\mathbf{q}, \boldsymbol{\tau}_{\mathrm{tot}})$ and $(\mathbf{q}, \dot{\mathbf{q}})$ are the coordinate representations of τ_{tot} and $\dot{q}$. The fact that robot manipulators are passive with respect to this input/output pair is well known. This property has been exploited by many researchers in deriving the so called *passivity based* trajectory following control laws for robot manipulator [4], [5], [9], [10].

With a feedback controller in place, the closed loop system can also be considered as an input-output system with the external force τ_e being the input and the velocity $\dot{q}$ being the output (Fig. 3). We can define the supply rate of this input/output system to be the power generated by the external

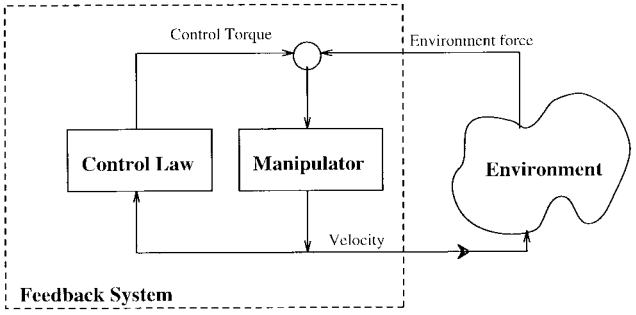

Fig. 3. Robot interacts with the environment and control.

force: $s(\tau_e, \dot{q}) = \boldsymbol{\tau}_e^T \dot{\mathbf{q}}$. Under a timed trajectory tracking control law, such as any of the *passivity based* control laws in [4], [5], [9], [10], the passivity relation

$$\int_0^t \boldsymbol{\tau}_e^T \dot{\mathbf{q}}\, d\tau \geq -c^2 \tag{3}$$

(where the supply rate is the power generated by the external force) cannot be guaranteed! The expression in (3) states that the net energy that can be transferred from the closed loop system to the environment is limited by c^2. As an illustration, consider a robot tracking a trajectory when it encounters an obstacle which brings the robot to rest. All the kinetic energy of the robot is thus absorbed by the obstacle (the environment). Suppose now that the obstacle is removed so that the robot resumes tracking the trajectory. It encounters a second obstacle which again brings the robot to rest. Since this procedure can be repeated infinitely, the environment can therefore absorb an infinite amount of energy, thus showing that the robot control system is not passive. Indeed, most timed trajectory tracking controllers in the robotics literature do not preserve the passivity of the closed loop system when the external forces are considered the input and the manipulator velocity the output. Notice that (3) is preserved in the absence of control, i.e. $\tau \equiv 0$.

In this paper we present a new control law for manipulators whose tasks are encoded by velocity fields and in addition guarantees the closed loop passivity relation given in (3). In Section II, we formally define our control objective and discuss several possible applications within this context. In Section III, the passive velocity field control (PVFC) law is derived. The properties of PVFC are presented in Section IV. A simulation example which illustrates the properties of the control law is given in Section V. Experimental results in the context of a contour following task are presented in Section VI. Concluding remarks are contained in Section VII. Most of the results contained in this paper were first presented in [11].

II. Problem Definition

Consider a mechanical manipulator with a n dimensional configuration manifold $\mathcal{G} = \{q\}$. It is subjected to controlled actuator forces $\tau \in T^*\mathcal{G}$ and to external forces $\tau_e \in T^*\mathcal{G}$ such as disturbances and contact forces. The manipulator is fully actuated so that τ can be arbitrarily assigned. Let $\mathbf{q} = [q_1, \ldots, q_n]^T$ denote a set of local coordinates for the manipulator configuration $q \in \mathcal{G}$, and $(\mathbf{q}, \boldsymbol{\tau})$ with $\boldsymbol{\tau} = [\tau^1, \ldots \tau^n]^T$, and $(\mathbf{q}, \boldsymbol{\tau}_e)$ with $\boldsymbol{\tau}_e = [\tau_e^1, \ldots \tau_e^n]^T$ denote the coordinate representations of the control force τ and external force τ_e, respectively. In these notations, the dynamics of the manipulator is given by the well known formula

$$\mathbf{M}(\mathbf{q})\ddot{\mathbf{q}} + \mathbf{C}(\mathbf{q}, \dot{\mathbf{q}})\dot{\mathbf{q}} = \boldsymbol{\tau} + \boldsymbol{\tau}_e \tag{4}$$

where the (r, s) element of $\mathbf{C}(\mathbf{q}, \boldsymbol{\zeta}) \in \Re^{n \times n}$ is given by

$$C_{rs}(\mathbf{q}, \boldsymbol{\zeta}) = \frac{1}{2} \sum_{t=1}^{n} \left[\frac{\partial M_{rs}}{\partial q_t} \zeta_t + \frac{\partial M_{tr}}{\partial q_s} \zeta_t - \frac{\partial M_{ts}}{\partial q_r} \zeta_t \right]$$

for any $\boldsymbol{\zeta} = [\zeta_1, \ldots, \zeta_n]^T \in \Re^n$. $\mathbf{M}(\mathbf{q}) \in \Re^{n \times n}$ is the inertia matrix and $M_{rs}(\mathbf{q})$ is its (r, s) element. In (4), we consider only the inertial dynamics. Dissipative and potential forces (like gravity) are treated as part of the external force $\boldsymbol{\tau}_e$.

In order to make our presentation clearer to the robotics community, all the results will be derived using the more familiar coordinate representation. The notational conventions used in this paper are given in the beginning of the paper. The readers are referred to [3], [12]–[14] for a development of this theory using coordinate independent notation.

In this paper, the following problem is solved:

Control Problem:

For the mechanical manipulator dynamics in (4), given the desired velocity field with the coordinate representation $\mathbf{V}(\mathbf{q})$, *find a control law for* $\boldsymbol{\tau}$ *such that*

1) *The feedback system in Fig. 3, with the external forces* $\boldsymbol{\tau}_e$ *as the input, and the manipulator's velocity* $(\mathbf{q}, \dot{\mathbf{q}})$ *as the output, is passive w.r.t. the supply rate* $s(\boldsymbol{\tau}_e, \dot{\mathbf{q}}) := \boldsymbol{\tau}_e^T \dot{\mathbf{q}}$. *i.e., there exists a* $c \in \Re$, *that may depend on the initial conditions, such that, for all* $t \geq 0$, *and for any external input force* $\boldsymbol{\tau}_e$, *(3) is satisfied;*
2) *In the absence of external forces, i.e.,* $\boldsymbol{\tau}_e \equiv \mathbf{0}$, *for any initial condition* $(\mathbf{q}(\mathbf{0}), \dot{\mathbf{q}}(\mathbf{0}))$, *there exists a constant* $\alpha > 0$ *s.t.*

$$\lim_{t \to \infty} [\dot{\mathbf{q}}(t) - \alpha \mathbf{V}(\mathbf{q}(t))] = \mathbf{0}.$$

The second specification stipulates that the velocity $\dot{\mathbf{q}}(t)$ converges to a scaled multiple of the desired velocity $\mathbf{V}(\mathbf{q}(t))$. As will be subsequently derived, the parameter α is a function of the total energy in the robot and control system.

Many robotic applications, such as robotic assembly and machining operations, require physical contacts with the environment. Since the environments are often strictly passive objects that dissipate energy, the passivity theorem [15] guarantees that the interaction between the closed loop robot control system which is also passive (as specified in control problem above) and these environments will be stable. Thus, the stability and robustness of these applications will be enhanced. By the same token, robotic devices such as robotic exercise machines, teleoperated manipulators, and rehabilitation machines must interact with human users closely. Safety of these systems are critical. When the closed loop robotic system is constrained to be passive, the amount of energy that may injure the human user in an accident will be limited. Thus, the safety of these devices can also be enhanced. In fact, the

control law that will be presented in this paper was originally developed to control smart exercise machines [16], [17].

Notice that in the problem formulation above, the specification of the task, as encoded by the velocity field, and that of the speed at which the task is performed, are decoupled. The proposed controller ensures that the task is performed, while the speed at which the task is accomplished is determined by the amount of energy in the system. This decoupling property of the control scheme may be useful in machining operations such as robotic deburring. In deburring, the deburring tool must follow a specified contour as fast as possible without being damaged. Thus, by solving the passive velocity field control problem for a velocity field which encodes the desired contour, we can ensure that the contour is followed regardless of the speed; while a secondary feedback loop can then be designed to control the energy (and hence the speed) of the system based on the monitored tool force.

III. Passive Velocity Field Control (PVFC)

The state space formulation of the passivity property of a dynamic system involves the definition of a storage function, which is a positive valued function of the system's state. Following [7], a dynamic system with input $u \in \mathcal{U}$ and output $y \in \mathcal{Y}$ and state $x \in \mathcal{X}$ is passive w.r.t. the supply rate $s : \mathcal{U} \times \mathcal{Y} \to \Re$, if a storage function $W : \mathcal{X} \to \Re_+$ exists s.t. for any initial state $x_0 \in \mathcal{X}$, any input function $u : \Re_+ \to \mathcal{U}$, and any $t > 0$,

$$\int_0^t s(u(\tau), y(\tau))\, d\tau \geq W(x(t)) - W(x_0), \tag{5}$$

where $x(t)$ is the state at time t. Since $W(\cdot) \geq 0$, this condition implies the passivity condition given in Definition 1 with $c^2 = W(x_0)$.

For mechanical systems, the total energy of the system is a natural candidate for storage function $W(\cdot)$. In the absence of potential energy, the total energy is simply the kinetic energy of the system.

Consider the situation when an appropriate control input $\boldsymbol{\tau}$ has been applied so that a scaled multiple α of the desired velocity field is exactly tracked—i.e., $\dot{\mathbf{q}} = \alpha \mathbf{V}(\mathbf{q})$. Even if the external force $\boldsymbol{\tau}_e$ is zero, the kinetic energy of the system at time t, $W(x(t))$ can typically exceed the initial kinetic energy $W(x_0)$ unless $\alpha = 0$. Thus, the passivity relation in (5) will not generally be satisfied with the supply rate given by $s(\boldsymbol{\tau}_e, \dot{q}) = {\boldsymbol{\tau}_e}^T \dot{\mathbf{q}}$, and the storage function $W(x(t))$ given by the kinetic energy. Therefore, the feedback system in Fig. 3 cannot generally be shown to be passive w.r.t. this supply rate. To overcome this difficulty, we define a new kinetic energy function for the closed loop control system and then design the controller so that it does not cause the new kinetic energy of the system to increase. This is done in three steps.

1) The original system is augmented with an extra state (the fictitious state) in order to incorporate the dynamics of an extra fictitious energy storage element. Subsequently, a kinetic energy function is defined for the augmented system. The fictitious state is interpreted to be the velocity of a fictitious flywheel in this paper.
2) An augmented *desired* velocity field for the augmented system is defined such that when it (or a multiple of it) is exactly tracked, the kinetic energy of the augmented system still remains constant.
3) The dynamics of the fictitious state (i.e., the flywheel velocity) and the original system are coupled in such a way that the augmented desired velocity field will be tracked while maintaining the kinetic energy of the augmented system to be constant.

The resulting passive velocity field controller (PVFC) obtained this way is a dynamic controller which does not generate any energy, but is capable of storing and releasing it. Since the input to the controller is the manipulator velocity $(\mathbf{q}, \dot{\mathbf{q}})$ and the output is the generalized force $\boldsymbol{\tau}$, the controller has the causality of a nonlinear dynamical impedance.

A. Augmented Mechanical System

Define the configuration space for an augmented mechanical system to be the $n+1$ dimensional manifold $\bar{\mathcal{G}} = \mathcal{G} \times S^1$ where the unit circle S^1 is interpreted to be the configuration space of a flywheel with inertia $M_F > 0$. The configuration of the augmented mechanical system will be denoted by $\bar{q} \in \bar{\mathcal{G}}$, with local coordinate representation given by

$$\bar{\mathbf{q}} = [\underbrace{q_1, \ldots, q_n}_{\mathbf{q}^T}, q_{n+1}]^T.$$

The dynamics of the flywheel is given by

$$M_F \ddot{q}_{n+1} = \tau^{n+1} \tag{6}$$

where τ_{n+1} is the coupling control input to the flywheel, which will be defined later on. Thus, the dynamics of the augmented system are given by

$$\bar{\mathbf{M}}(\bar{\mathbf{q}})\ddot{\bar{\mathbf{q}}} + \bar{\mathbf{C}}(\bar{\mathbf{q}}, \dot{\bar{\mathbf{q}}})\dot{\bar{\mathbf{q}}} = \bar{\boldsymbol{\tau}} + \bar{\boldsymbol{\tau}}_e \tag{7}$$

where $(\bar{\mathbf{q}}, \dot{\bar{\mathbf{q}}})$ with $\dot{\bar{\mathbf{q}}} = [\dot{\mathbf{q}}^T \ \ \dot{q}_{n+1}]^T \in \Re^{n+1}$ is the velocity of the augmented system, $(\bar{\mathbf{q}}, \bar{\boldsymbol{\tau}})$ with $\bar{\boldsymbol{\tau}} = [\boldsymbol{\tau}^T \ \ \tau^{n+1}]^T \in \Re^{n+1}$ is the augmented control input, $(\bar{\mathbf{q}}, \bar{\boldsymbol{\tau}}_e)$ with $\bar{\boldsymbol{\tau}}_e = [\boldsymbol{\tau}_e^T \ \ 0]^T \in \Re^{n+1}$ is the augmented external force, all expressed in local coordinates, and

$$\bar{\mathbf{M}}(\bar{\mathbf{q}}) = \begin{bmatrix} \mathbf{M}(\mathbf{q}) & 0 \\ 0 & M_F \end{bmatrix}, \quad \bar{\mathbf{C}}(\bar{\mathbf{q}}, \dot{\bar{\mathbf{q}}}) = \begin{bmatrix} \mathbf{C}(\mathbf{q}, \dot{\mathbf{q}}) & 0 \\ 0 & 0 \end{bmatrix}$$

are the augmented inertia matrix and Coriolis matrix.

For each augmented configuration $\bar{q} \in \bar{G}$, we define the kinetic energy of the augmented dynamic system $\bar{k} : T_{\bar{q}}\bar{\mathcal{G}} \to \Re$, expressed in local coordinates by

$$\bar{k}(\bar{\mathbf{q}}, \dot{\bar{\mathbf{q}}}) = \frac{1}{2} \dot{\bar{\mathbf{q}}}^T \bar{\mathbf{M}}(\bar{\mathbf{q}}) \dot{\bar{\mathbf{q}}}. \tag{8}$$

B. Augmented Desired Velocity Field $\bar{V}$

Recall that the desired velocity field $V : \mathcal{G} \to T\mathcal{G}$ assigns a desired velocity at every point q in the manipulator's configuration space and is designed so that if $\dot{q} = \alpha V(q)$, the manipulator would execute the desired task. The speed at which the manipulator executes the desired task is dictated by the constant $\alpha \in \Re$. For the augmented mechanical system, an

augmented desired velocity field $\bar{V} : \bar{\mathcal{G}} \to T\bar{\mathcal{G}}$ is needed. It is defined so that the following condition is satisfied:

Condition 1: The augmented desired velocity field $\bar{V} : \bar{\mathcal{G}} \to T\bar{\mathcal{G}}$ satisfies:

Conservation of kinetic energy: The total kinetic energy of the augmented system evaluated at the **desired** velocity field $\bar{V}(\bar{q})$ is constant, i.e. in local coordinates the following condition is satisfied for all $\bar{q} \in \bar{\mathcal{G}}$:

$$\bar{k}(\bar{\mathbf{q}}, \bar{\mathbf{V}}(\bar{\mathbf{q}})) = \frac{1}{2}\bar{\mathbf{V}}(\bar{\mathbf{q}})^T \bar{\mathbf{M}}(\bar{\mathbf{q}})\bar{\mathbf{V}}(\bar{\mathbf{q}}) = \bar{E} > 0 \tag{9}$$

where $\bar{E}$ is a positive scalar.

Consistency: The component of the augmented velocity field that corresponds to the original manipulator should be the same as the specified desired velocity field, i.e., $\bar{\mathbf{V}}(\bar{\mathbf{q}})$ is of the form

$$\bar{\mathbf{V}}(\bar{\mathbf{q}}) = [\mathbf{V}(\mathbf{q})^T, V_{n+1}(\mathbf{q})]^T. \tag{10}$$

Condition 1 implies that $\bar{\mathbf{V}}(\bar{\mathbf{q}})$ can be defined by first specifying a $\bar{E}$ and then by determining the desired velocity field for the fictitious inertia $V_{n+1}(\mathbf{q})$ in (10) using

$$V_{n+1}(\mathbf{q}) = \sqrt{\frac{2}{M_F}\left(\bar{E} - \frac{1}{2}\mathbf{V}(\mathbf{q})^T \mathbf{M}(\mathbf{q})\mathbf{V}(\mathbf{q})\right)}. \tag{11}$$

Notice that $\bar{E}$ should be selected to be large enough so that (11) has a real solution. It should now be apparent that the fictitious inertia acts as a reservoir of kinetic energy.

C. Coupling Control Law

Recall that $\bar{q}$, $\dot{\bar{q}}$ are the the position and velocity of the augmented system, while $\bar{V}(\bar{q})$ is the desired augmented velocity field. To facilitate the presentation of the coupling control law, we denote $\bar{p} \in T^*\mathcal{G}$ to be the momentum of the augmented system, $\bar{P} \in T^*\mathcal{G}$ to be the desired momentum of the augmented system and $\bar{w} \in T^*\mathcal{G}$ to be the momentum associated with the co-variant derivative of the desired velocity with respect to the actual manipulator velocity. This last object is normally denoted as $\bar{M}\nabla_{\dot{\bar{q}}}\bar{V}$, where the connection used in calculating the co-variant derivative is the Levi-Civita connection associated with the inertia $\bar{M}(\bar{q})$ [2], [8]. It can be shown that $\bar{M}\nabla_{\dot{\bar{q}}}\bar{V} = \nabla_{\dot{\bar{q}}}\bar{P}$, the covariant derivative of the desired momentum [2]. The coordinate representation of these objects are

$$\bar{\mathbf{p}}(\bar{\mathbf{q}}, \dot{\bar{\mathbf{q}}}) = \bar{\mathbf{M}}(\bar{\mathbf{q}})\dot{\bar{\mathbf{q}}} \tag{12}$$

$$\bar{\mathbf{P}}(\bar{\mathbf{q}}) = \bar{\mathbf{M}}(\bar{\mathbf{q}})\bar{\mathbf{V}}(\bar{\mathbf{q}}) \tag{13}$$

$$\bar{\mathbf{w}}(\bar{\mathbf{q}}, \dot{\bar{\mathbf{q}}}) = \bar{\mathbf{M}}(\bar{\mathbf{q}})\dot{\bar{\mathbf{V}}}(\bar{\mathbf{q}}) + \bar{\mathbf{C}}(\bar{\mathbf{q}}, \dot{\bar{\mathbf{q}}})\bar{\mathbf{V}}(\bar{\mathbf{q}}) \tag{14}$$

where the i-th component of $\dot{\bar{\mathbf{V}}}$ is

$$\dot{\bar{V}}_i(\bar{\mathbf{q}}) = \sum_{k=1}^{n+1} \frac{\partial \bar{V}_i(\bar{\mathbf{q}})}{\partial \bar{q}_k}\dot{\bar{q}}_k. \tag{15}$$

As will be detailed subsequently, $\bar{w}$ is the inverse dynamics necessary to follow the augmented desired velocity field.

The coupling control law in (7) is given by

$$\bar{\boldsymbol{\tau}}(\bar{\mathbf{q}}, \dot{\bar{\mathbf{q}}}) = \bar{\boldsymbol{\tau}}_c(\bar{\mathbf{q}}, \dot{\bar{\mathbf{q}}}) + \bar{\boldsymbol{\tau}}_f(\bar{\mathbf{q}}, \dot{\bar{\mathbf{q}}}) \tag{16}$$

where

$$\bar{\boldsymbol{\tau}}_c = \underbrace{\frac{1}{2\bar{E}}(\bar{\mathbf{w}}\bar{\mathbf{P}}^T - \bar{\mathbf{P}}\bar{\mathbf{w}}^T)}_{\text{skew symmetric}}\dot{\bar{\mathbf{q}}} \tag{17}$$

$$\bar{\boldsymbol{\tau}}_f = \gamma\underbrace{(\bar{\mathbf{P}}\bar{\mathbf{p}}^T - \bar{\mathbf{p}}\bar{\mathbf{P}}^T)}_{\text{skew symmetric}}\dot{\bar{\mathbf{q}}}. \tag{18}$$

The $\bar{\mathbf{q}}, \dot{\bar{\mathbf{q}}}$ arguments in $\bar{\mathbf{p}}$ and $\bar{\mathbf{w}}$ as well as the $\bar{\mathbf{q}}$ argument in $\bar{\mathbf{P}}$ have been omitted to avoid clutter. $\gamma \in \Re$ in (18) is a control gain, not necessarily positive, which determines the convergence rate and the sense in which the desired velocity field will be followed.

The coupling control law in (16)–(18) can also be written in coordinate invariant notation as

$$\bar{\tau} = \dot{\bar{q}} \rfloor \left\{ \bar{P} \wedge \left(\frac{1}{2\bar{E}} \bar{M} \nabla_{\dot{\bar{q}}} \bar{V} - \gamma \bar{p} \right) \right\} \tag{19}$$

where $\wedge$ is the wedge product for differential forms and $\rfloor$ is the contraction operator [2]. The readers are referred to [3], [12], and [13] for details.

As a comparison between the coupling control law in (16)–(18) with other model based robot tracking controllers in the literature (such as in [10], [18], and [19]), consider a passivity based control law for tracking the augmented desired velocity field which is of the form[1]

$$\bar{\boldsymbol{\tau}}_{ct}(\bar{\mathbf{q}}, \dot{\bar{\mathbf{q}}}) = \bar{\mathbf{w}}(\bar{\mathbf{q}}, \dot{\bar{\mathbf{q}}}, t) + \mathbf{K}[\bar{\mathbf{V}}(\bar{\mathbf{q}}, t) - \dot{\bar{\mathbf{q}}}] \tag{20}$$

where $\mathbf{K}$ is a positive definite feedback gain matrix (see the passivity based control scheme by Slotine and Li in [4] or the ECCL in [5] for details).

The control laws in (16)–(18) and in (20) are similar in that they both consist of an inverse dynamic term [$\bar{\boldsymbol{\tau}}_c$ in (17), $\bar{\mathbf{w}}$ in (20)] and a stabilizing feedback term [$\bar{\boldsymbol{\tau}}_f$ in (18), $\mathbf{K}[\bar{\mathbf{V}}(\bar{\mathbf{q}}, t) - \dot{\bar{\mathbf{q}}}]$ in (20)]. However, there are also significant differences. For example, the coupling control $\boldsymbol{\tau}(\mathbf{q}, \dot{\mathbf{q}})$ is quadratic in the velocity in the sense that $\boldsymbol{\tau}(\mathbf{q}, \alpha\dot{\mathbf{q}}) = \alpha^2\boldsymbol{\tau}(\mathbf{q}, \dot{\mathbf{q}})$ whereas the passivity based controller (20) is typically affine in $\dot{\mathbf{q}}$. As we shall see, the two types of controllers also have very different closed loop properties. For instance, with the coupling control (16)–(18), the closed loop dynamics remain passive with respect to the supply rate $\boldsymbol{\tau}_e^T\dot{\mathbf{q}}$ which is not the case when the passivity based controller (20) is used. Moreover, when external forces are absent (i.e., $\boldsymbol{\tau}_e \equiv \mathbf{0}$), the passivity based controller will achieve $\dot{\mathbf{q}}(t) \to \mathbf{V}(\mathbf{q}(t), t)$. On the other hand, the coupling control will achieve $\dot{\mathbf{q}}(t) \to \alpha\mathbf{V}(\mathbf{q}(t))$ where the parameter α is a function of the total energy of the closed loop system which needs not be defined a-priori. In this case, the speed at which the desired velocity field is tracked depends on the energy available in the system which can be increased or extracted using the external input $\boldsymbol{\tau}_e$.

IV. Rationale and Properties of PVFC

We now discuss the rationale behind the formulation of the passive velocity field control (PVFC) law.

[1] Equation (20) is presented for comparison purposes only since the use of an augmented state is not necessary in passivity based control schemes. Also, the velocity field to be tracked is typically time varying such as as defined using (2).

A. Skew Symmetric Structure of the Control Law

The skew symmetric structure of the control terms in (17) and (18) is necessary to preserve the passivity of the feedback system w.r.t. the supply rate given by the power produced by the external forces, while achieving the desired tracking action. To show this fact, define the skew symmetric matrices

$$\mathbf{G}(\bar{\mathbf{q}},\dot{\bar{\mathbf{q}}}) = \frac{1}{2\bar{E}}(\bar{\mathbf{w}}\bar{\mathbf{P}}^T - \bar{\mathbf{P}}\bar{\mathbf{w}}^T) \tag{21}$$

$$\mathbf{R}(\bar{\mathbf{q}},\dot{\bar{\mathbf{q}}}) = (\bar{\mathbf{P}}\bar{\mathbf{p}}^T - \bar{\mathbf{p}}\bar{\mathbf{P}}^T). \tag{22}$$

Notice that the $\bar{\mathbf{q}}$ and $\dot{\bar{\mathbf{q}}}$ arguments on the right hand side of (21)–(22) have again been omitted to avoid clutter. With this notation, the closed loop dynamics for the coupled augmented system can be written in local coordinates as

$$\bar{\mathbf{M}}(\bar{\mathbf{q}})\ddot{\bar{\mathbf{q}}} + \bar{\mathbf{Y}}(\bar{\mathbf{q}},\dot{\bar{\mathbf{q}}})\dot{\bar{\mathbf{q}}} = \bar{\tau}_e \tag{23}$$

where $\bar{\tau}_e$ is the coordinate representation for the augmented external force and the matrix $\bar{\mathbf{Y}} \in \Re^{(n+1)\times(n+1)}$ is given by

$$\bar{\mathbf{Y}}(\bar{\mathbf{q}},\dot{\bar{\mathbf{q}}}) = \bar{\mathbf{C}}(\bar{\mathbf{q}},\dot{\bar{\mathbf{q}}}) - \mathbf{G}(\bar{\mathbf{q}},\dot{\bar{\mathbf{q}}}) - \gamma\mathbf{R}(\bar{\mathbf{q}},\dot{\bar{\mathbf{q}}}). \tag{24}$$

Notice that since both $\mathbf{G}$ and $\mathbf{R}$ are skew symmetric, $\dot{\bar{\mathbf{M}}} - 2\bar{\mathbf{Y}}$ is also skew symmetric, just as $\dot{\mathbf{M}} - 2\mathbf{C}$ is skew symmetric for the robot manipulator.

Proposition 1: The closed loop dynamics of the augmented system, which is given by (23), is passive with respect to the supply rate $\tau_e^T\dot{\mathbf{q}}$ (the power produced by the external forces), and its kinetic energy defined in (8) is its storage function.

Proof: Notice that, since $\bar{\tau}_e = [\tau_e^T \;\; 0]^T$, $\bar{\tau}_e^T\dot{\bar{\mathbf{q}}} = \tau_e^T\dot{\mathbf{q}}$. Differentiating (8), utilizing (23) and the fact that $\dot{\bar{\mathbf{M}}} - 2\bar{\mathbf{Y}}$ is skew symmetric we obtain

$$\frac{d}{dt}\bar{k}(\bar{\mathbf{q}}(t),\dot{\bar{\mathbf{q}}}(t)) = \tau_e^T(t)\dot{\mathbf{q}}(t). \tag{25}$$

The result follows by integrating (25) w.r.t. time. □

B. Augmented State

As discussed earlier, the augmented state, which is interpreted as the velocity of a fictitious inertia in this paper, plays the role of a reservoir of kinetic energy. The addition of this state to the control law makes it possible for the kinetic energy of the augmented system to remain constant when the augmented velocity is a multiple of the augmented desired velocity field. This is to ensure that the passivity property of the closed loop system with respect to the supply rate $\tau_e^T\dot{\mathbf{q}}$ will not be violated. It is so as long as the kinetic energy of the augmented desired velocity field is constant [see (9)]. Notice that (9) cannot generally be satisfied without the additional state.

As a consequence of the energy conservation condition in (9), the following lemma states that the inverse dynamics compensation term $\bar{w} = \nabla_{\dot{\bar{q}}}\bar{P} = \bar{M}\nabla_{\dot{\bar{q}}}\bar{V}$ with local coordinate representation given by (14), always annihilates the desired velocity field $\bar{V}$.

Lemma 1: If the desired augmented velocity field $\bar{V} : \bar{\mathcal{G}} \to T\bar{\mathcal{G}}$ is defined such that it satisfies (9), then in any local coordinate representation, the inverse dynamic compensation term $\bar{\mathbf{w}}(\bar{\mathbf{q}},\dot{\bar{\mathbf{q}}})$ in (14) satisfies

$$\bar{\mathbf{w}}^T(\bar{\mathbf{q}},\dot{\bar{\mathbf{q}}})\bar{\mathbf{V}}(\bar{\mathbf{q}}) = 0. \tag{26}$$

Proof: Taking the time derivative of (9), we obtain

$$\dot{\bar{k}}(\bar{\mathbf{q}}(t),\bar{\mathbf{V}}(\bar{\mathbf{q}}(t))) = \dot{\bar{E}} = 0. \tag{27}$$

Evaluating the left hand side of (27) we obtain

$$\begin{aligned} 0 &= \frac{1}{2}\frac{d}{dt}\{\bar{\mathbf{V}}^T(\bar{\mathbf{q}})\bar{\mathbf{M}}(\bar{\mathbf{q}})\bar{\mathbf{V}}(\bar{\mathbf{q}})\} \\ &= \bar{\mathbf{V}}^T(\bar{\mathbf{q}})\left\{\frac{1}{2}\dot{\bar{\mathbf{M}}}(\bar{\mathbf{q}})\bar{\mathbf{V}}(\bar{\mathbf{q}}) + \bar{\mathbf{M}}(\bar{\mathbf{q}})\dot{\bar{\mathbf{V}}}(\bar{\mathbf{q}})\right\} \\ &= \bar{\mathbf{V}}^T(\bar{\mathbf{q}})\{\bar{\mathbf{M}}(\bar{\mathbf{q}})\dot{\bar{\mathbf{V}}}(\bar{\mathbf{q}}) + \bar{\mathbf{C}}(\bar{\mathbf{q}},\dot{\bar{\mathbf{q}}})\bar{\mathbf{V}}(\bar{\mathbf{q}})\} \\ &= \bar{\mathbf{V}}^T(\bar{\mathbf{q}})\bar{\mathbf{w}}(\bar{\mathbf{q}},\dot{\bar{\mathbf{q}}}) \end{aligned}$$

where we have used the definition of $\bar{\mathbf{w}}$ given by (14) and the fact that the matrix $\dot{\bar{\mathbf{M}}}(\bar{\mathbf{q}}) - 2\bar{\mathbf{C}}(\bar{\mathbf{q}},\dot{\bar{\mathbf{q}}})$ is skew symmetric. □

Loosely speaking, Lemma 1 can be interpreted as follows. Since the inverse dynamics compensation $\bar{\mathbf{w}}(\bar{\mathbf{q}},\dot{\bar{\mathbf{q}}})$ acts in the normal direction to the desired velocity field $\bar{\mathbf{V}}(\bar{\mathbf{q}})$, it is responsible for steering the system to negotiate along the integral curves of the augmented desired velocity field $\bar{\mathbf{V}}(\bar{\mathbf{q}})$, but not in changing the speed along the curves.

C. Coupling Control Term $\bar{\tau}_c$ in (17)

In order to further study the velocity field tracking properties of the augmented mechanical feedback system, it will be helpful to define the augmented $\alpha-$ velocity error. For *any* $\alpha \in \Re$, the local coordinate representation of the augmented $\alpha-$ velocity error $\bar{e}_\alpha$ is defined by $(\bar{\mathbf{q}},\bar{\mathbf{e}}_\alpha)$ where

$$\bar{\mathbf{e}}_\alpha := \dot{\bar{\mathbf{q}}} - \alpha\bar{\mathbf{V}}(\bar{\mathbf{q}}). \tag{28}$$

Notice that the velocity field tracking requirement will be satisfied if $\bar{\mathbf{e}}_\alpha(t) \to 0$ for some α.

The following proposition shows that the role of the coupling control $\bar{\tau}_c$ in (16), which is given by (17), is to make the whole *family* of augmented $\alpha-$ velocity error dynamics with any α, passive. This role is analogous to the role of the inverse dynamics compensation term $\bar{\mathbf{w}}$ in the passivity based control law (20), in making the reference velocity error $\bar{e} = \dot{\bar{q}} - \bar{V}(\bar{q})$ dynamics passive [18], [19].

Proposition 2: For any $\alpha \in \Re$, the augmented $\alpha-$ velocity error dynamics is passive with respect to the supply rate $(\bar{\tau}_f + \bar{\tau}_e)^T\bar{\mathbf{e}}_\alpha$, with the storage function being

$$W_\alpha(\bar{\mathbf{q}},\bar{\mathbf{e}}_\alpha) := \frac{1}{2}\bar{\mathbf{e}}_\alpha^T\bar{\mathbf{M}}(\bar{\mathbf{q}})\bar{\mathbf{e}}_\alpha. \tag{29}$$

Proof: Adding the term $-\alpha\bar{\mathbf{w}}$ to both sides of (4) we obtain

$$\bar{\mathbf{M}}(\bar{\mathbf{q}})\dot{\bar{\mathbf{e}}}_\alpha + \bar{\mathbf{C}}(\bar{\mathbf{q}},\dot{\bar{\mathbf{q}}})\bar{\mathbf{e}}_\alpha = -\alpha\bar{\mathbf{w}} + \bar{\tau}_c + \bar{\tau}_f + \bar{\tau}_e.$$

Using Lemma 1, (17), and some algebra we obtain

$$\begin{aligned}-\alpha\bar{\mathbf{w}} + \bar{\tau}_c &= -\alpha\bar{\mathbf{w}} + \frac{1}{2\bar{E}}(\bar{\mathbf{w}}\bar{\mathbf{P}}^T - \bar{\mathbf{P}}\bar{\mathbf{w}}^T)\dot{\bar{\mathbf{q}}} \\ &= \frac{1}{2\bar{E}}(\bar{\mathbf{w}}\bar{\mathbf{P}}^T - \bar{\mathbf{P}}\bar{\mathbf{w}}^T)\bar{\mathbf{e}}_\alpha.\end{aligned}$$

Thus

$$\bar{\mathbf{M}}(\bar{\mathbf{q}})\dot{\bar{\mathbf{e}}}_\alpha + (\bar{\mathbf{C}}(\bar{\mathbf{q}},\dot{\bar{\mathbf{q}}}) - \mathbf{G}(\bar{\mathbf{q}},\dot{\bar{\mathbf{q}}}))\bar{\mathbf{e}}_\alpha = \bar{\tau}_f + \bar{\tau}_e \tag{30}$$

where the skew symmetric matrix $\mathbf{G}$ is defined in (21) and $\bar{\tau}_f$ is the second term in the coupling control law (16). Differentiating (29), utilizing (30) and the fact that $\dot{\bar{\mathbf{M}}} - 2(\bar{\mathbf{C}} - \mathbf{G})$ is skew symmetric, we obtain

$$\frac{d}{dt}W_\alpha(\bar{\mathbf{q}}(t),\bar{\mathbf{e}}_\alpha(t)) = (\bar{\tau}_f + \bar{\tau}_e)^T\bar{\mathbf{e}}_\alpha. \tag{31}$$

The result follows by integrating (31) with respect to time. □

D. Coupling Control Term $\bar{\tau}_f$ in (18)

The role of the coupling control term $\bar{\tau}_f$ in (16) is to cause the $\alpha-$ velocity error dynamics to converge. This role is analogous to that of the feedback term $-\mathbf{K}[\dot{\bar{\mathbf{q}}} - \bar{\mathbf{V}}(\bar{\mathbf{q}})]$ in the passivity based control law (20) in stabilizing the dynamics of the tracking error $\bar{e} = \dot{\bar{q}} - \bar{V}(\bar{q})$. This is necessary for the velocity of the augmented system to converge to a multiple of the augmented desired velocity field in the absence of external forces.

To see that this is indeed the case, let us evaluate $\bar{\mathbf{e}}_\alpha^T\bar{\tau}_f$, which determines the effect of $\bar{\tau}_f$ on the storage function $W_\alpha(\bar{\mathbf{q}},\bar{\mathbf{e}}_\alpha)$ in (29) in Proposition 2

$$\begin{aligned}\bar{\mathbf{e}}_\alpha^T\bar{\tau}_f &= \bar{\mathbf{e}}_\alpha^T\gamma\mathbf{R}\dot{\bar{\mathbf{q}}} = -\alpha\gamma\bar{\mathbf{V}}^T\mathbf{R}\dot{\bar{\mathbf{q}}} \\ &= -\alpha\gamma\{(\bar{\mathbf{V}}^T\bar{\mathbf{M}}\bar{\mathbf{V}})(\dot{\bar{\mathbf{q}}}^T\bar{\mathbf{M}}\dot{\bar{\mathbf{q}}}) - (\bar{\mathbf{V}}^T\bar{\mathbf{M}}\dot{\bar{\mathbf{q}}})^2\}\end{aligned} \tag{32}$$

where we have utilized the definition of the matrix $\mathbf{R}$ in (22) and, to avoid clutter, the $\bar{\mathbf{q}}$ and $\dot{\bar{\mathbf{q}}}$ argument in the expressions have been omitted.

It can be easily verified from Schwartz's inequality (for $\forall\mathbf{v},\mathbf{u}\in\Re^n$, $(\mathbf{v}^T\mathbf{u})^2 \le (\mathbf{v}^T\mathbf{v})\cdot(\mathbf{u}^T\mathbf{u})$) and the fact that $\bar{\mathbf{M}}$ is positive definite, that $[(\bar{\mathbf{V}}^T\bar{\mathbf{M}}\bar{\mathbf{V}})(\dot{\bar{\mathbf{q}}}^T\bar{\mathbf{M}}\dot{\bar{\mathbf{q}}}) - (\bar{\mathbf{V}}^T\bar{\mathbf{M}}\dot{\bar{\mathbf{q}}})^2]$ is nonnegative. Thus

$$\bar{\mathbf{e}}_\alpha^T\bar{\tau}_f\begin{cases}\le 0, & \text{if } \alpha\gamma > 0 \\ \ge 0, & \text{if } \alpha\gamma < 0 \\ = 0, & \text{if } \alpha\gamma = 0 \quad \text{or} \quad \text{if } \exists\lambda\in\Re, \quad \text{s.t. } \dot{\bar{\mathbf{q}}} = \lambda\bar{\mathbf{V}}\end{cases}. \tag{33}$$

Therefore, combining (33) and (31), we see that the effect of $\bar{\tau}_f$ is to decrease the storage function W_α whenever $\alpha\gamma > 0$ and the velocity $\dot{\bar{\mathbf{q}}}$ is not yet aligned with the desired velocity field $\bar{\mathbf{V}}$.

E. Main Results

We are now ready to state our main result.

Theorem 1: Consider the feedback system in Fig. 3 where the manipulator is given by (4), and the PVFC control law consists of the dynamic augmentation (6) and the coupling control law (16)–(18). Let the external force $\tau_e \in T^*\mathcal{G}$ be the input and the velocity $\dot{q}\in T\mathcal{G}$ be the output of the feedback system.

1) The kinetic energy of the augmented system $\bar{k}(\bar{\mathbf{q}},\dot{\bar{\mathbf{q}}})$ in (8) satisfies
$$\frac{d}{dt}\bar{k}(\bar{\mathbf{q}}(t),\dot{\bar{\mathbf{q}}}(t)) = \boldsymbol{\tau}_e^T(t)\dot{\mathbf{q}}(t).$$
2) The feedback system is passive w.r.t. the supply rate $s(\boldsymbol{\tau}_e,\dot{q}) = \boldsymbol{\tau}_e{}^T\dot{\mathbf{q}}$ in the sense of Definition 1.
3) Suppose that the external force is absent, i.e., $\boldsymbol{\tau}_e \equiv \mathbf{0}$. Let α be <u>any</u> real number. If the feedback gain γ in (18) is chosen so that $\gamma\alpha \ge 0$, then the solution
$$\bar{\mathbf{e}}_\alpha := \dot{\bar{\mathbf{q}}} - \alpha\bar{\mathbf{V}}(\bar{\mathbf{q}}) = \mathbf{0}$$
is a Lyapunov stable equilibrium of the error dynamics (30).
4) Assume again that $\boldsymbol{\tau}_e \equiv \mathbf{0}$ and define the constant $\beta\in\Re$ such that
$$\beta^2 = \bar{k}(\bar{\mathbf{q}},\dot{\bar{\mathbf{q}}})/\bar{E} \tag{34}$$
where $\bar{E} = \bar{k}(\bar{\mathbf{q}},\bar{\mathbf{V}})$ is given in (9). The solution
$$\bar{\mathbf{e}}_\beta = \dot{\bar{\mathbf{q}}} - \beta\bar{\mathbf{V}}(\bar{\mathbf{q}}) = \mathbf{0}$$
is a globally exponentially stable equilibrium of the error dynamics (30) if $\gamma\beta > 0$ except for a set of initial conditions with measure zero. It is exponentially unstable if $\gamma\beta < 0$. In the neighborhood of $\bar{\mathbf{e}}_\beta = \mathbf{0}$, the rate of exponential convergence ($\gamma\beta > 0$) or divergence ($\gamma\beta < 0$) is given by 2 $\gamma\beta\bar{E}$.

Proof: Parts 1. and 2. are restatements of Proposition 1. □

Proof of Part 3: Given $\alpha\in\Re$, let W_α be the positive definite storage function defined in (29). We shall use the notations $W_\alpha(t)$ and $W_\alpha(\bar{\mathbf{q}}(t),\dot{\bar{\mathbf{q}}}(t))$ interchangeably. From (31) in the proof of Proposition 2

$$\begin{aligned}\frac{d}{dt}W_\alpha(t) &= \bar{\mathbf{e}}_\alpha^T\bar{\tau}_f + \bar{\mathbf{e}}_\alpha^T\bar{\tau}_e \\ &= -\alpha\gamma\cdot[4\bar{k}(\bar{\mathbf{q}},\dot{\bar{\mathbf{q}}})\bar{E} - (\bar{\mathbf{V}}^T\bar{\mathbf{M}}\dot{\bar{\mathbf{q}}})^2] + \bar{\mathbf{e}}_\alpha^T\bar{\tau}_e\end{aligned} \tag{35}$$

where (35) is obtained from (32) and by substituting the expressions in (9) and (8). In the case when $\bar{\tau}_e \equiv 0$ and $\alpha\cdot\gamma > 0$, in light of (33), (35) becomes

$$\frac{d}{dt}W_\alpha(t) = \bar{\mathbf{e}}_\alpha^T\bar{\tau}_f \le 0.$$

Since $W_\alpha(\bar{\mathbf{q}}(t),\bar{\mathbf{e}}_\alpha(t))$ is a positive definite function of $\bar{\mathbf{e}}_\alpha$, $\bar{\mathbf{e}}_\alpha = \mathbf{0}$ is Lyapunov stable.

Proof of Part 4: Let β be as defined in (34). By setting $\alpha = \beta$ in (35) and by utilizing (34) and the identity $(a^2 - b^2) = (a - b)(a + b)$, we obtain

$$\frac{d}{dt}W_\beta = -\beta \cdot \gamma[4\beta^2 \bar{E}^2 - (\bar{\mathbf{V}}\bar{\mathbf{M}}\dot{\bar{\mathbf{q}}})^2] + \bar{\boldsymbol{\tau}}_e^T \bar{\mathbf{e}}_\beta$$
$$= -\gamma \cdot \beta(2\beta\bar{E} - \bar{\mathbf{V}}^T\bar{\mathbf{M}}\dot{\bar{\mathbf{q}}})(2\beta\bar{E} + \bar{\mathbf{V}}^T\bar{\mathbf{M}}\dot{\bar{\mathbf{q}}}) + \bar{\boldsymbol{\tau}}_e^T \bar{\mathbf{e}}_\beta. \tag{36}$$

On the other hand, using (28) and (34), we obtain for any $\alpha \in \Re$,

$$W_\alpha = \frac{1}{2}\bar{\mathbf{e}}_\alpha^T \bar{\mathbf{M}}\bar{\mathbf{e}}_\alpha = (\beta^2 + \alpha^2)\bar{E} - \alpha\bar{\mathbf{V}}^T\bar{\mathbf{M}}\dot{\bar{\mathbf{q}}} \tag{37}$$

so that by setting $\alpha = \beta$ in (37), we obtain

$$\frac{W_\beta}{\beta} = 2\beta\bar{E} - \bar{\mathbf{V}}^T\bar{\mathbf{M}}\dot{\bar{\mathbf{q}}}. \tag{38}$$

Hence, (36) becomes

$$\frac{d}{dt}W_\beta = -\gamma W_\beta[2\beta\bar{E} + \bar{\mathbf{V}}^T\bar{\mathbf{M}}\dot{\bar{\mathbf{q}}}] + \bar{\boldsymbol{\tau}}_e^T \bar{\mathbf{e}}_\beta$$
$$= -4\gamma\beta\bar{E} \cdot \mu(t) \cdot W_\beta + \bar{\boldsymbol{\tau}}_e^T \bar{\mathbf{e}}_\beta \tag{39}$$

where

$$\mu(t) := \frac{1}{2}\left[1 + \frac{\bar{\mathbf{V}}^T(\bar{\mathbf{q}}(t))\bar{\mathbf{M}}(\bar{\mathbf{q}}(t))\dot{\bar{\mathbf{q}}}(t)}{2\beta\bar{E}}\right]. \tag{40}$$

Notice that $0 \le \mu(t) \le 1$ since, by Schwartz's inequality, $|\bar{\mathbf{V}}^T\bar{\mathbf{M}}\dot{\bar{\mathbf{q}}}| \le 2|\beta|\bar{E}$. Moreover, $\mu \to 1$ as $\bar{\mathbf{e}}_\beta \to \mathbf{0}$.

Suppose now that $\bar{\boldsymbol{\tau}}_e \equiv \mathbf{0}$. Then, by Proposition 1, $\bar{k}(\bar{\mathbf{q}}(t), \dot{\bar{\mathbf{q}}}(t))$, and hence, $\beta(t)$ are constants. Thus, from (39), and by differentiating (40), we have

$$\frac{d}{dt}W_\beta(t) = -4\gamma\beta\bar{E} \cdot \mu(t) \cdot W_\beta(t) \tag{41}$$

$$\frac{d}{dt}\mu(t) = +\frac{\gamma\beta}{\beta^2} \cdot \mu(t) \cdot W_\beta(t). \tag{42}$$

Equation (42) is obtained by utilizing (38) and recognizing that β is a constant before differentiating (40), and finally by substituting the $\dot{W}_\beta$ term that results with (41).

Consider first the case when $\gamma\beta > 0$. Because $\mu(t) \ge 0$ and $W_\beta(t) \ge 0$, (42) shows that $\mu(t)$ is nondecreasing. Thus (41) becomes

$$\frac{d}{dt}W_\beta(t) \le -4\gamma\beta\bar{E} \cdot \mu(0) \cdot W_\beta(t)$$

showing that $W_\beta \to 0$ exponentially from any initial conditions $(\bar{\mathbf{q}}(0), \bar{\mathbf{e}}_\beta(0))$ so that $\mu(0) \neq 0$. Hence, $\bar{\mathbf{e}}_\beta \to \mathbf{0}$ exponentially at a rate $\ge 2\gamma\beta\mu(0)\bar{E}$. The set of initial conditions that make $\mu(0) = 0$ is exactly given by the set of unstable equilibria characterized by $\bar{\mathbf{e}}_{-\beta}(0) = \mathbf{0}$, i.e., $\dot{\bar{\mathbf{q}}}(0) = -\beta\bar{\mathbf{V}}(\bar{\mathbf{q}}(0))$, which is of measure 0 . This shows that for the case of $\gamma\beta > 0$, the equilibria $\bar{\mathbf{e}}_\beta = \mathbf{0}$ is globally exponentially stable from all initial conditions except for the unstable equilibrium state $\bar{\mathbf{e}}_{-\beta}(0) = \mathbf{0}$. Moreover, in the neighborhood of $\bar{\mathbf{e}}_\beta = \mathbf{0}$, $\mu(t) \approx 1$ so $\bar{\mathbf{e}}_\beta \to \mathbf{0}$ at an exponential rate of $2\gamma\beta\bar{E}$ in the neighborhood of $\bar{\mathbf{e}}_\beta = \mathbf{0}$.

By considering $t \to -\infty$, a similar argument shows that in the case of $\gamma\beta < 0$, $\bar{\mathbf{e}}_\beta(0) = \mathbf{0}$ is exponentially unstable. □

Remarks:

1) Notice that β in (34) is proportional to the square root of the kinetic energy in the system. Thus, the magnitude of the velocity $|\dot{\bar{\mathbf{q}}}|$ and β are linearly related. It is interesting to note that the exponential rate of convergence of $\bar{\mathbf{e}}_\beta$ is also linear with β. If time is scaled by $1/\beta$, then the closed loop dynamics (23) become normalized and independent of β.
2) As remarked in the introduction, the proposed controller encodes an entire class of behaviors of the manipulator specified by the ODE $\dot{\bar{\mathbf{q}}} = \alpha\bar{\mathbf{V}}(\bar{\mathbf{q}})$, where α is an arbitrary constant which can be positive or negative. In this way, the natural behavior of the closed loop feedback system in the absence of external disturbances, is to trace out the integral curves of the ODE, in the same manner that the natural behavior of a particle in free space is to travel in straight lines. The magnitude and sign of the specific α adopted (hence the speed and the sign of the motion) are determined by the available energy in the system and the sign of the feedback gain γ respectively. Notice that the role of the coupling control $\bar{\boldsymbol{\tau}}_f$ in (18) is to align $\dot{\bar{\mathbf{q}}}$ in the direction of the desired velocity field $\bar{\mathbf{V}}(\bar{\mathbf{q}})$. This suggests that two very different behaviors can be encoded by a single velocity field with one executed when the feedback gain $\gamma > 0$ and the other when $\gamma < 0$. An example for this application is presented in Section V.
3) The controller formulation presented in Section III can be used to design timed trajectory tracking controllers if we define the *time varying* desired velocity field $V(q, t)$ given by (1). In such a case, (9) and (11), which respectively determine the desired total energy of the augmented system and the desired velocity field of the augmented state, must still be satisfied. (Notice that (9) is a necessary condition for Lemma 1.) Additionally, (15) must be modified as

$$\dot{\bar{V}}_i(\bar{\mathbf{q}}, t) = \sum_{k=1}^{n+1} \frac{\partial \bar{V}_i(\bar{\mathbf{q}}, t)}{\partial \bar{q}_k}\dot{\bar{q}}_k + \frac{\partial \bar{V}_i(\bar{\mathbf{q}}, t)}{\partial t}. \tag{43}$$

Thus, as in other timed trajectory tracking controllers, the timed trajectories of the desired configuration $Q(t)$, velocity $\dot{Q}(t)$ and acceleration $\ddot{Q}(t)$ must be available to the control system. The passive velocity field control (PVFC) law will cause $\dot{\mathbf{q}} \to \beta\mathbf{V}(\mathbf{q}, t)$. However, if $\mathbf{V}$ is obtained from a desired trajectory $Q(t)$ via (1) and it is desired that $q(t) \to Q(t)$, then it is also necessary to have the correct amount of kinetic energy, i.e., $\beta = 1$.
4) The passive velocity field control formulation presented in this paper can be extended and generalized to the problem of tracking parameterized curves of the form $Q : \mathcal{I} \to \mathcal{G}$, where $\mathcal{I} \in \Re$ is the domain of the parameterization and $\mathcal{G}$ is the manipulator's configuration manifold. Interested readers are referred to [3], [12], and [14], where the controller is formulated using *dynamic time suspension*. This extension is important for contour following applications as it bypasses the potentially

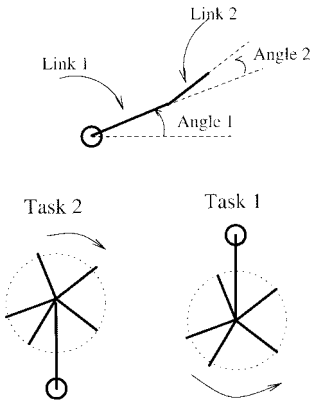

Fig. 4. Two-link manipulator and the two tasks encoded by the velocity in Fig. 5.

tricky step of designing an appropriate velocity field to encode a contour.

V. Two-Task Encoding Example

In this example, we illustrate the possibility to encode two dynamic tasks using one velocity field, and the use of the proposed passive velocity field controller for their stabilization. Consider a two link SCARA manipulator with a configuration space of $S^1 \times S^1$. Assume that the robot moves in the horizontal plane so that gravitational force can be neglected. We specify two tasks for the robot (Fig. 4).

Task 1: The second link spins (in the anti-clockwise sense) at angular velocity $V_2 = 1 + 0.5\cos(q_2)$ while the first link stabilizes at position 1.5 π;

Task 2: The second link spins (in the clockwise sense) at angular velocity $V_2 = -1 - 0.5\cos(q_2)$ while the first link stabilizes at position 0.5 π.

The velocity field in Fig. 5 encodes *both* tasks simultaneously: Task 1 is executed when the velocity field is tracked in the forward sense, and Task 2 is executed when the field is tracked in the backward sense. The sign of the feedback gain γ in (16) will determine which task will be performed.

We set the initial configuration to be $q_1(0) = \pi$ rad, $q_2(0) = 0$ rad, and the initial velocities to be $\dot{q}_1(0) = 10$ rad/s, $\dot{q}_2(0) = 0$ rad/s. The initial velocity of the fictitious flywheel is 0. Suppose that the external force is $\tau_e = [20, 0]^T$ Nm, which is active during the interval $t \in [8, 12]$ s and is otherwise 0. We set the gain γ to be 0.1 when $t \leq 20$ s and $\gamma = -0.1$ when $t > 20$ s. As a consequence, Task 1 should be performed for $t < 20$ s and Task 2 should be performed for $t > 20$ s.

The time duration of the simulation is 30 s. In Fig. 5, the actual angles and the desired velocity fields are superimposed. Notice that the manipulator quickly converges to perform Task 1 in the first portion of the simulation. During the period $t \in [8, 12]$ s when the external force is active, the robot deviates from Task 1 as link 1 becomes offset from the desired angle of 1.5 π. When the external force becomes inactive again, Task 1 is again stabilized. Finally, when the gain γ is switched to -0.1 ($t = 20$ s), the robot converges to Task 2, however at a higher speed than in the beginning of the simulation. In this simulation, the magnitude of the feedback gain $|\gamma|$ is deliberately set to a small value to exaggerate the effect of the environment force on the performance of the system. Fig. 6 shows the superimposed snapshots of the configurations of the robot during the three time intervals: [0,8], [8,12], and [12,30].

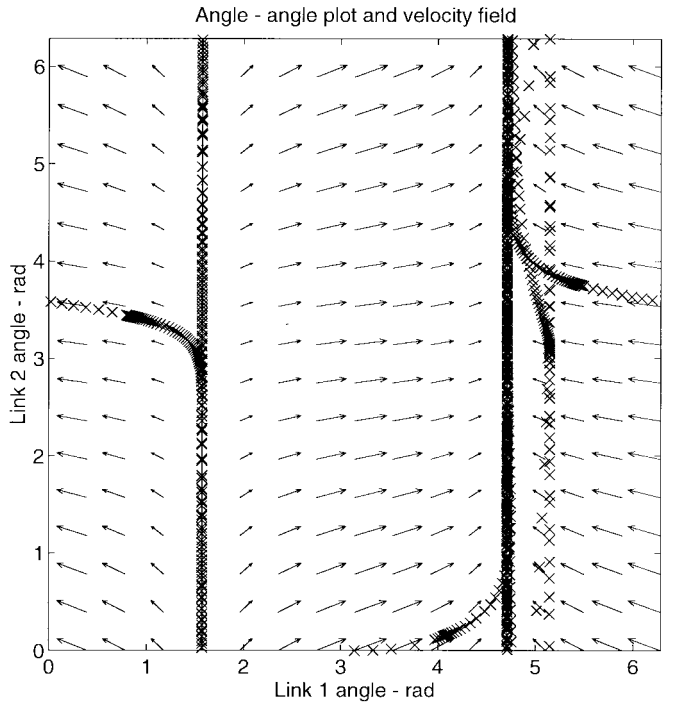

Fig. 5. Velocity field that encodes the tasks in Fig. 4 superimposed by the plot of $q_2(t)$ versus $q_1(t)$ obtained from the simulation.

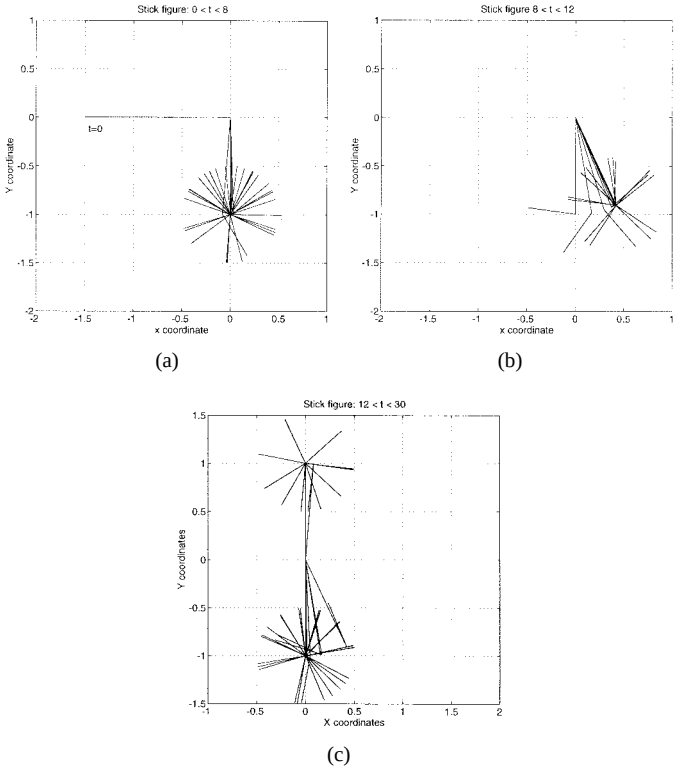

Fig. 6. Stick figure plots. (a) Task 1 is satisfied for $t < 8$ s. (b) Deviation from Task 1 for $8 < t < 12$ s due to external forces. (c) For $t > 12$ s Task 1 is satisfied initially and then Task 2 is satisfied after γ switches sign.

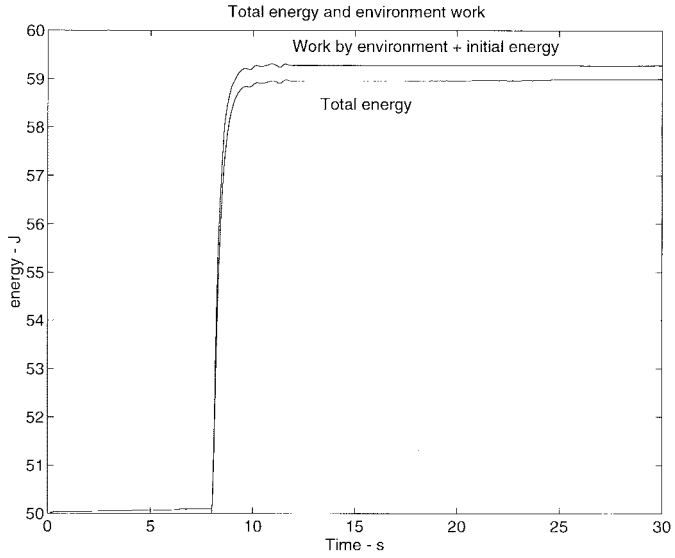

Fig. 7. Total energy and external energy input + initial energy.

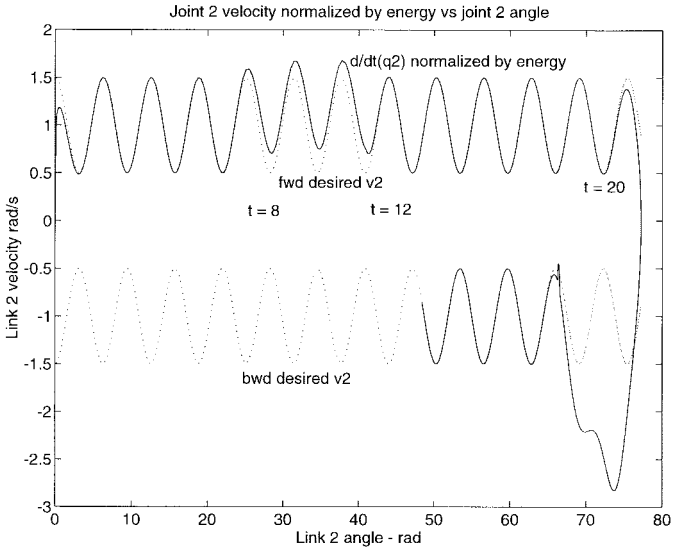

Fig. 8. Normalized link 2 velocity: $\frac{\dot{q}_2}{|\beta|}$ where $\beta^2 = \bar{k}(\bar{\mathbf{q}}, \dot{\bar{q}})/\bar{E}$ and $\bar{V}^2$.

Fig. 7 shows the changes in total energy. The energy remains constant for $t < 8$ s and $t > 12$ s. During the period $t \in [8, 12]$ s the external force performs active work on the robot, thus the total energy increases. The discrepancy between the environment energy input and the change in total energy is due to discretization. Fig. 8 shows the velocity $\dot{q}_2(t)$ of link 2 and the position $q_2(t)$. Here, $\dot{q}_2(t)/|\beta(t)|$ is plotted against $q_2(t)$ where β^2 is the ratio between the total energy $(\bar{k})$ in the system at time t and $\bar{E}$ in (9). Notice that the normalized velocity follows either $+V_2(\mathbf{q}(t))$ or $-V_2(\mathbf{q}(t))$, except during the period when the external force is active.

VI. Contour Following Experiments

In this section we present experimental results which show the Berkeley/NSK two link direct drive SCARA manipulator following a circular contour in joint space. A detailed description of this manipulator can by found in [20]. We compare the response of the Berkeley/NSK arm under PVFC and a nonadaptive model based timed trajectory control law, known as the desired compensation control law (DCCL) [5]. The adaptive version of the DCCL has been shown to perform superiorly to other adaptive model based trajectory tracking controllers [21]. The desired circular contour was centered at the origin of the joint coordinate space and had a radius of 1. The desired velocity field was designed so that if $\dot{\bar{\mathbf{q}}} = \mathbf{V}(\bar{\mathbf{q}}(t))$, then the contour would be followed at an angular contouring velocity of 1 rad/s. In all experiments, joint friction was partially compensated by adding to both the PVCF and the DCCL the following control action:

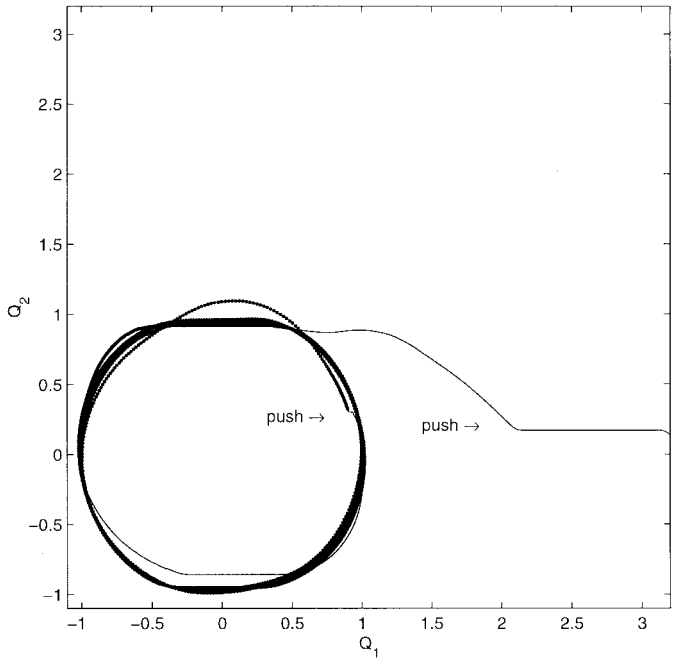

Fig. 9. Robot tracking a unit circular contour under PVFC.

$$\tau_1 = c_1 \cdot \mathrm{sgn}(\dot{q}_1), \quad \tau_2 = c_2 \cdot \mathrm{sgn}(\dot{q}_2) \tag{44}$$

where c_1 and c_2 are estimates of the magnitude of the joint Coulomb friction. It should be emphasized that the same control gains were used between experiment runs, and no attempt was done to adjust the gains of either controller to optimize performance. Thus, the objective of this study is primarily to illustrate the properties that set PVFC apart from model based timed trajectory controllers, and not to compare their performances.

In the first experiment, performed using PVFC only, the fictitious flywheel was given a small amount of initial angular speed. The robot was manually pushed twice during the experiment to increase its kinetic energy. As shown in Fig. 9, the robot quickly tracked the desired circular contour after it gained sufficient kinetic energy. Moreover, even when it is being manually pushed, the robot tends to follow the circular contour. In effect, it appears that tracing the unit circle becomes the robot's "*natural*" motion under PVFC. Notice from Fig. 10, that the contouring angular speed

$$\omega = \sqrt{\frac{\dot{\mathbf{q}}^T \dot{\mathbf{q}}}{\mathbf{q}^T \mathbf{q}}}$$

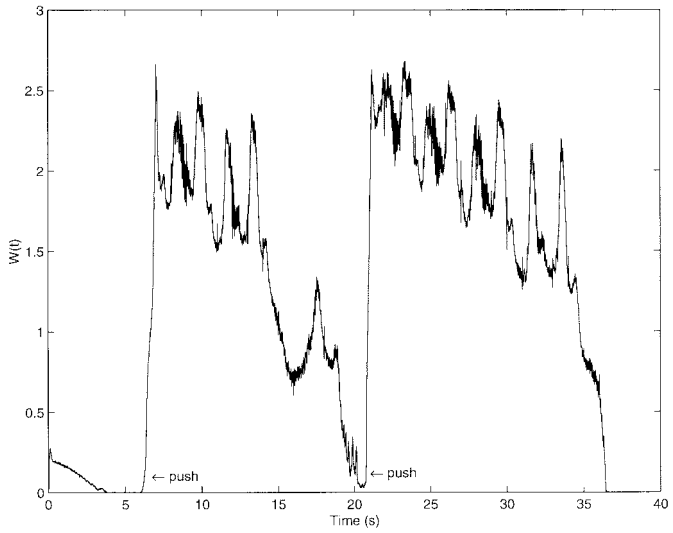

Fig. 10. Contouring angular speed.

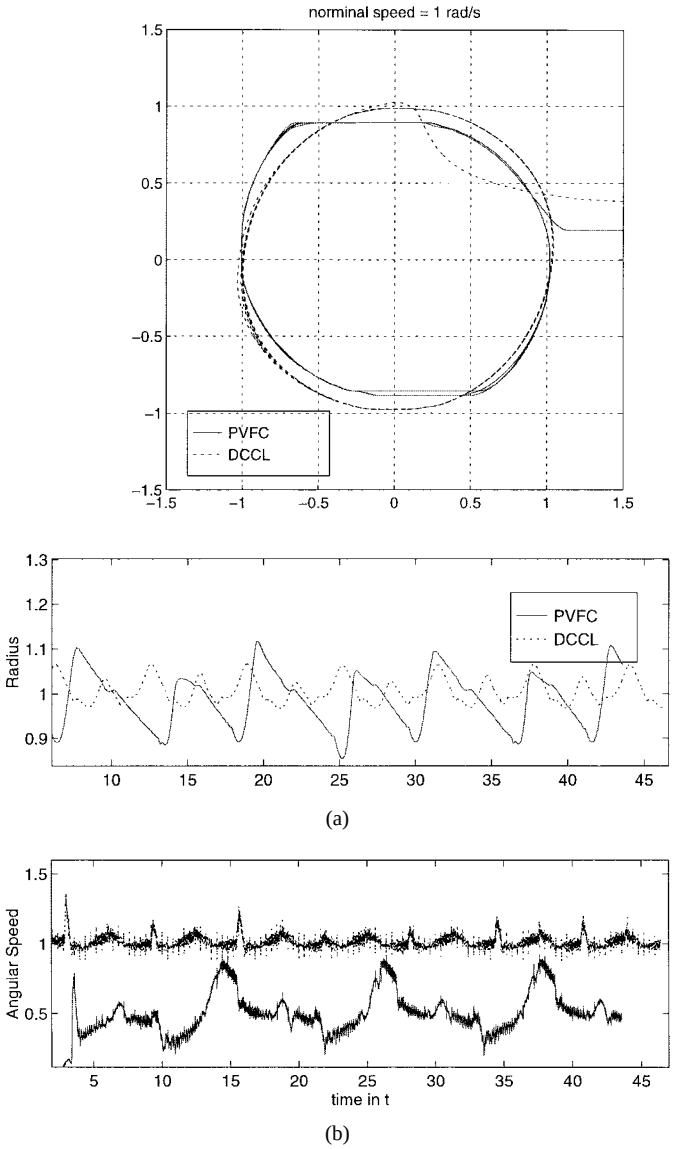

(a)

(b)

Fig. 11. Contour traced by robot under DCCL and PVFC control. The commanded speed is 1 rad/s. (a) Contour traced. (b) Radius and angular speed.

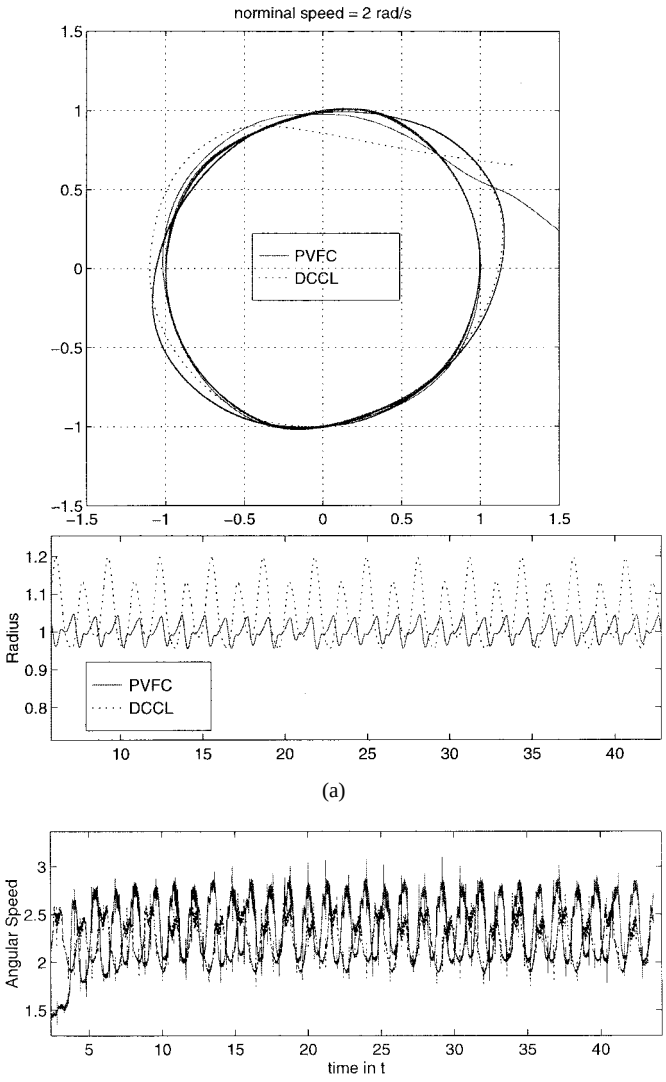

(a)

(b)

Fig. 12. Contour traced by robot under DCCL and PVFC control. The commanded speed is 2 rad/s. (a) Contour traced. (b) Radius and angular speed.

increases every time that the robot is manually pushed. Since the friction compensation terms in (44) were not set to a sufficiently high value to overcome the actual joint friction, the energy of the robot decreases as it performs the contour tracking. Because the DCCL is not closed loop passive, it is not safe to manually push the robot while it is following the contour under this control law. This is the case with most model based trajectory following controllers.

In the second experiment, the robot was commanded to follow the circular contour at contouring angular speeds of 1 rad/s, 2 rad/s and 3 rad/s, respectively. In order to regulate the contour following speed when using the PVFC, the additional term

$$\bar{\tau}_f = -\delta \bar{\mathbf{P}}(\bar{\mathbf{q}}) \left[\omega_d - \frac{[\bar{\mathbf{P}}^T(\bar{\mathbf{q}})\dot{\bar{\mathbf{q}}}]}{2\bar{E}} \right] \tag{45}$$

was also added to the coupling control (16), where $\bar{\mathbf{P}}(\bar{\mathbf{q}})$ is given in (13), ω_d is the desired contouring angular speed while following the circle, and $\delta = 0.5$ is a small damping coefficient. Since the desired velocity field was designed so

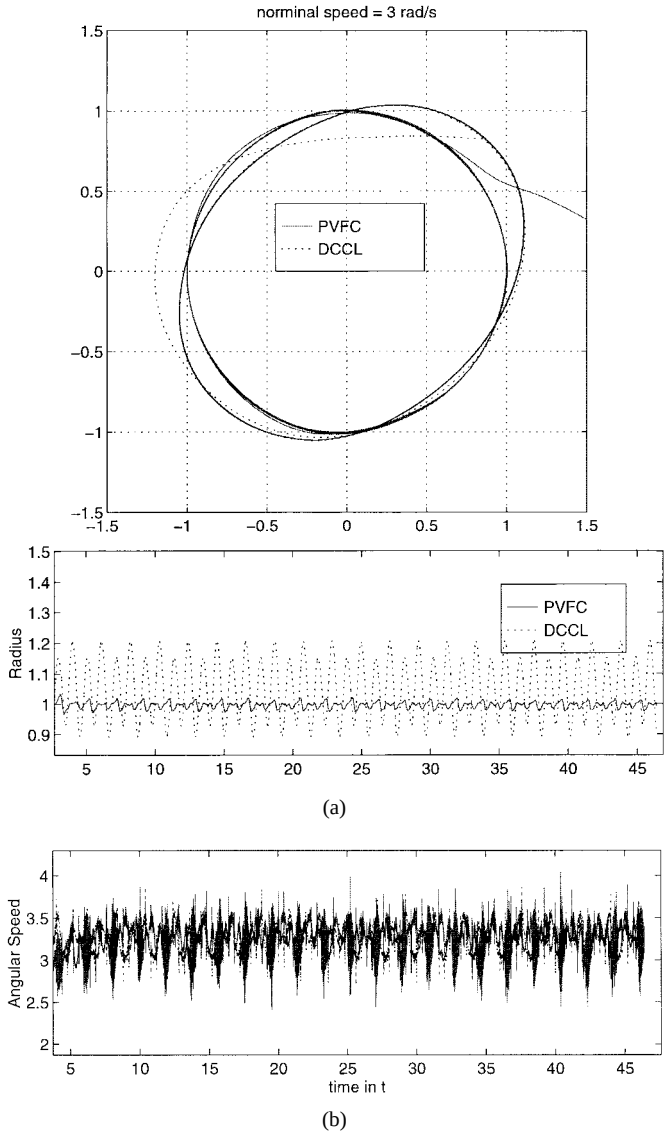

Fig. 13. Contour traced by robot under DCCL and PVFC control. The commanded speed is 3 rad/s. (a) Contour traced. (b) Radius and angular speed.

that the circular contour is followed at an angular contouring velocity of 1 rad/s when the robot satisfies the ODE $\dot{\bar{\mathbf{q}}} = \mathbf{V}(\bar{\mathbf{q}}(t))$, if the robot satisfies the ODE $\dot{\bar{\mathbf{q}}} = \omega_d \bar{\mathbf{V}}(\dot{\bar{\mathbf{q}}})$ it will follow the contour at a contouring angular speed ω_d. Under this control law, taking $\alpha = \omega_d$, the dynamics of the Lyapunov function W_{ω_d}, which was previously given by (35), becomes

$$\frac{d}{dt}W_{\omega_d} = -\omega_d \gamma \cdot [4\bar{k}(\bar{\mathbf{q}}, \dot{\bar{\mathbf{q}}})\bar{E} - (\bar{\mathbf{V}}^T \bar{\mathbf{M}} \dot{\bar{\mathbf{q}}})^2] - \frac{\delta}{2\bar{E}}\left(\bar{\mathbf{e}}_{\omega_d}^T \bar{\mathbf{P}}\right)^2. \tag{46}$$

Thus, it can be concluded that $\dot{\bar{\mathbf{q}}}(t) \to \omega_d \bar{\mathbf{V}}(\bar{\mathbf{q}}(t))$.

As shown in Figs. 11–13, the performance of the DCCL controller deteriorated as the contour following speed increased, whereas that of the PVFC actually *improved*. In particular, at 1 rad/s, the DCCL outperformed the PVFC. However, at 2 rad/s and at 3 rad/s, the PVFC outperformed the DCCL. An analysis of this rather nonintuitive robustness result can be found in [12] and [13]. Notice also that, at the commanded speed of 1 rad/s, the effect of the uncompensated stiction was very evident, and the actual following speed is much lower than the commanded speed.

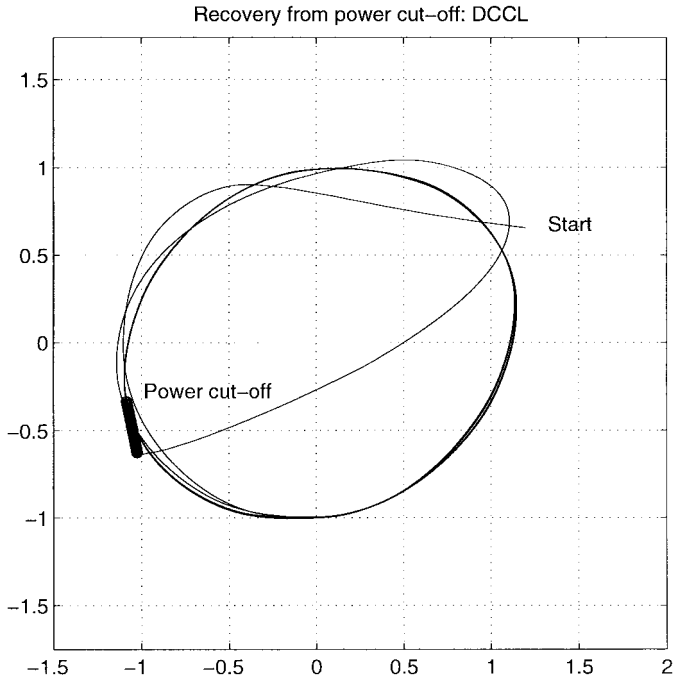

Fig. 14. Contour traced by robot under DCCL. Torque inputs were set to zero for a period of 1 s in the middle of the experiment.

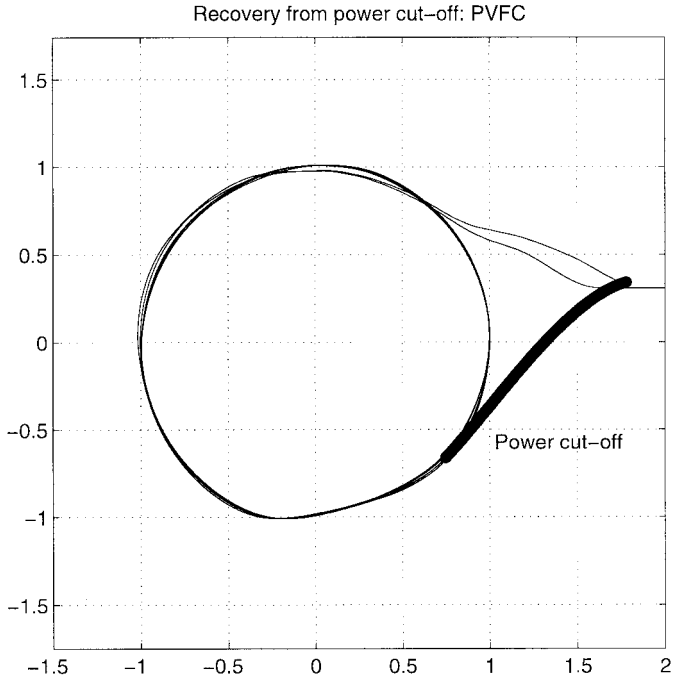

Fig. 15. Contour traced by robot under PVFC. Torque inputs were set to zero for a period of 1 s in the middle of the experiment.

In the third experiment, we investigated how the DCCL and the PVFC recovered from unforeseen disturbances or system faults. While the robot was tracking the circle, the torque inputs to the motors were set to zero for a period of 1 s in order to simulate a power outage. Fig. 14 shows the response of the robot under the DCCL, while Fig. 15 shows the response of the robot under the PVFC. Notice from Fig. 14, that after

power was restored and even though the actual robot position was very close to the contour, the DCCL controller caused to robot to move drastically away from the contour, in order to catch up with the timed trajectory. On the other hand, as shown in Fig. 15, under similar circumstances, the robot under PVFC returns to the contour, following a natural path. It should be noted that the state of the robot at the instant when the power outage occurs determines its subsequent movement, which is governed by the inertial dynamics and friction alone, until the control system is turned back on. In the case of Fig. 14, the momentum of the robot is relatively small at the point when the power outage started (the velocity of link 1, which is the massive link, was small). On the other hand, in the case of Fig. 15, the momentum of the robot was much higher at the instant when the power outage started. For this reason the robot moved much further during the power outage in the PVFC experiment, as shown in Fig. 15, than in the DCCL experiment shown in Fig. 14.

VII. Conclusion

In this paper, we developed a new passive velocity field controller for mechanical manipulators. The controller mimics the dynamics of a flywheel, so it does not generate energy. It is capable of tracking a scaled multiple of a desired velocity field. The resulting closed loop feedback system is passive when external forces are considered as the input, the manipulator velocity as the output, and the external mechanical power as the supply rate. Although we have used contour following to motivate the control scheme, other applications that have strong coordination and behavioral aspects, and require interaction with the physical environment may also be suitable. A simulation example which illustrates the behavior of the manipulator under this control law was presented. Experimental results that compare the proposed control law with the popular passivity based timed trajectory tracking control approach in the context of contour following were also presented. We have also applied and implemented the proposed controller to other applications, such as robot contour following problems which may not admit a definition of a desired velocity field [12]; to the control of smart exercise machines [16], [17]; and to the control of bilateral teleoperated manipulators [22]. In [12]–[14], additional geometric and robustness properties of the proposed controller can also be found.

References

[1] T. C. Chiu, "Coordination control of multiple axes mechanical system: Theory and experiments," Ph.D. dissertation, Dept. Mech. Eng., Univ. California, Berkeley, 1994.

[2] R. L. Bishop and S. I. Goldberg, *Tensor Analysis on Manifolds*. New York: Dover, 1980.

[3] P. Y. Li, "Self optimizing control and passive velocity field control of intelligent machines," Ph.D. dissertation, Dept. Mech. Eng., Univ. California, Berkeley, 1995.

[4] J. Slotine and W. Li, *Applied Nonlinear Control*. Englewood Cliffs, NJ: Prentice-Hall, 1991.

[5] N. Sadegh and R. Horowitz, "Stability and robustness analysis of a class of adaptive controllers for robotic manipulators," *Int. J. Robot. Res.*, vol. 9, no. 3, pp. 74–92, June 1990.

[6] T.-J. Tarn, N. Xi, and A. K. Bejczy, "Path-based approach to integrated planning and control for robotic systems," *Automatica*, vol. 32, pp. 1675–1687, 1996.

[7] J. C. Willems, "Dissipative dynamical systems, part 1: General theory," *Arch. Rational Mech. Anal.*, vol. 45, pp. 321–351, 1972.

[8] J. E. Marsden and T. S. Ratiu, *Introduction to Mechanics and Symmetry*. New York: Springer-Verlag, 1993, vol. I.

[9] R. Ortega and M. Spong, "Adaptive motion control of rigid robots: A tutorial," *Automatica*, pp. 877–888, Nov. 1989.

[10] The ZODIAC, *Theory of Robot Control*. New York: Springer-Verlag, 1996.

[11] P. Y. Li and R. Horowitz, "Passive velocity field control of mechanical manipulators," in *Proc. 1995 IEEE Int. Conf. Robot. Automat.*, Nagoya, Japan, Apr. 1995, vol. 3, pp. 2764–2770.

[12] ———, "Application of passive velocity field control to contour following problems," in *Proc. 1996 IEEE Conf. Decision Contr.*, Kobe, Japan, Dec. 1996, vol. 1, pp. 378–385.

[13] ———, "Passive velocity field control, part 1: Geometry and robustness," in *IEEE Trans. Automat. Contr.*, to be published.

[14] ———, "Passive velocity field control, part 2: Application to contour following problems," in *IEEE Trans. Automat. Contr.*, to be published.

[15] M. Vidyasagar, *Analysis of Nonlinear Dynamic Systems*, 2nd ed. Englewood Cliffs, NJ: Prentice-Hall, 1993.

[16] P. Y. Li and R. Horowitz, "Control of smart exercise machines, Part 1. Problem formulation and nonadaptive control," *IEEE/ASME Trans. Mechatron.*, vol. 2, pp. 237–247, Dec. 1997.

[17] ———, "Control of smart exercise machines, part 2. Self-optimizing control," *IEEE/ASME Trans. Mechatron.*, vol. 2, pp. 248–257, Dec. 1997.

[18] R. Horowitz, "Learning control of robot manipulators," *ASME J. Dyn. Syst., Meas., Contr.*, vol. 115, no. 2B, pp. 402–411, 1993.

[19] K. Kaneko and R. Harowitz, "Repetitive and adaptive control of robot manipulators with velocity estimation," *IEEE Trans. Robot. Automat.*, vol. 13, pp. 204–217, Apr. 1997.

[20] C. G. Kang, W. W. Kao, M. Boals, and R. Horowitz, "Modeling and identification of a two link SCARA manipulator," in *Proc. Symp. Robot., ASME Winter Annu. Meeting*, Chicago, IL, 1988, pp. 393–407.

[21] L. L. Whitcomb, A. A. Rizzi, and D. E. Koditschek, "Comparative experiments with a new adaptive controller for robot arms," *IEEE Trans. Robot. Automat.*, vol. 9, pp. 59–70, Feb. 1993.

[22] P. Y. Li, "Passive control of bilateral teleoperated manipuators," in *Proc. Amer. Contr. Conf.*, 1998, pp. 3838–3842.

Perry Y. Li (S'87–M'95) received the B.A. degree (with honors) in electrical and information sciences from Cambridge University, Cambridge, U.K. in 1987, the M.S. degree in biomedical engineering from Boston University, Boston, MA, in 1990, and the Ph.D. degree in mechanical engineering from the University of California at Berkeley in 1995.

After graduation, he worked as a Member of Research Staff at Xerox Corporation, Webster, NY, where he performed control system research for xerographic printers and media handling systems. Since 1997, he has been with the Department of Mechanical Engineering, University of Minnesota, Minneapolis, as the Nelson Assistant Professor. His research interests are in nonlinear and intelligent control systems with applications to man–machine systems, robotics, mechatronics, automated vehicle and highway traffic control, and biomedical devices.

Dr. Li received the Achievement and the Special Recognition awards from Xerox Corporation.

Roberto Horowitz (M'83) was born in Caracas, Venezuela in 1955. He received the B.S. degree (with highest honors) and the Ph.D. degree in mechanical engineering from the University of California at Berkeley, in 1978 and 1983, respectively.

In 1982, he joined the Department of Mechanical Engineering, University of California, Berkeley, where he is a Professor. He teaches and conducts research in the areas of adaptive, learning, nonlinear and optimal control, with applications to microelectromechanical systems (MEMS), computer disk file systems, robotics, mechatronics, and intelligent vehicle and highway systems (IVHS).

Dr. Horowitz received the 1984 IBM Young Faculty Development Award and the 1987 National Science Foundation Presidential Young Investigator Award. He is a member of ASME.